Available online at www.sciencedirect.com
ScienceDirect
Journal of Solid State Chemistry 180 (2007) 92–97
JOURNAL OF SOLID STATE CHEMISTRY
www.elsevier.com/locate/jssc

# Synthesis, structure and magnetic properties of *R*–W–O–N (*R* = Nd and Eu) oxynitrides

R. Pastrana-Fábregas[a], J. Isasi-Marín[a], C. Cascales[b], R. Sáez-Puche[a,*]

[a]*Department of Química Inorgánica I, Facultad de Ciencias Químicas, Universidad Complutense, 28040 Madrid, Spain*
[b]*Instituto de Ciencia de Materiales de Madrid ICMM, Consejo Superior de Investigaciones Científicas CSIC, C/ Sor Juana Inés de la Cruz, 3. Cantoblanco, 28040 Madrid, Spain*

Received 18 July 2006; received in revised form 28 September 2006; accepted 28 September 2006
Available online 4 October 2006

**Abstract**

Neodymium and europium tungsten oxynitrides have been synthesized by the nitridation of corresponding $R_2W_2O_9$ precursor oxides, in ammonia flow at 1173 K during 24 h. The obtained polycrystalline neodymium oxynitride phase, with $NdWO_{3.05}N_{0.95}$ composition, crystallizes with the tetragonal symmetry of the scheelite-type structure, space group S.G. $I4_1/a$ (#88). The analogous europium derivative, with formula $EuWO_{1.58}N_{1.42}$, presents the cubic perovskite-type structure, S.G. $Pm\bar{3}m$ (# 221). Unit-cell parameters, $a = 5.255(1)$ Å, $c = 11.399(3)$ Å, and $a = 3.976(3)$ Å, have been established from Rietveld refinements of collected X-ray powder diffraction patterns for the Nd and Eu- oxynitrides, respectively.

Magnetic susceptibility measurements show that $NdWO_{3.05}N_{0.95}$ behaves as paramagnetic in a wide range of temperature $T$ ~50–300 K. The downwards deviation from the Curie–Weiss law below 40 K reflects the splitting of the $^4I_{9/2}$ ground state of $Nd^{3+}$ experienced under the influence of a $S_4$ crystal field CF potential, as the successful reproduction of the magnetic susceptibility $\chi_m^{-1}$ vs. $T$, using semi-empirical structure-derived CF parameters, indicates. $EuWO_{1.58}N_{1.42}$ is paramagnetic down to 20 K, and the measured effective magnetic moment 8.01 $\mu_B$ is indicative of the presence of $Eu^{2+}$ in this oxynitride. The observed sudden jump in the magnetic susceptibility at 20 K and the value of 6 $\mu_B$ for the saturation moment is attributed to the onset of ferrimagnetic interactions in which the $Eu^{2+}$ and $W^{5+}$ sublattices appear to be involved.


*Keywords:* Oxynitrides; Scheelite; Ferrimagnetism; Crystal field simulation

## 1. Introduction

While most research efforts concerning with oxides have been focused on modifications of the cation composition, a less-explored approach is to investigate modifications of the anion composition.

From the oxides to oxynitrides, the anionic substitution of divalent oxygen for trivalent nitrogen causes an increase in the covalency of the *M*–O/N bonds giving rise to marked modification on the structural, transport, optical and magnetic properties of the resulting oxynitrides. These materials could be used in different applications such as ceramics, glasses and pigments [1,2].

Rare-earth quaternary oxynitrides *R*–*M*–O–N, where *R* is a rare earth and *M* is a metal transition element can be derived from the ternary *R*–*M*–O oxides by partially replacing oxygen by nitrogen. The possible combination of *R*/*M* elements together with the gradual variation of the oxygen/nitrogen ratio gives rise to a large number of new a quaternary oxynitrides. However, oxynitrides have been poorly studied although recently with the development of the new preparation methods and characterization procedures, the chemistry of the oxynitrides has experienced a remarkable advance.

The crystal structures and some properties of these quaternary oxynitrides have been reported by Marchand

*Corresponding author. Fax: +33 91 394 43 52.
*E-mail address:* rsp92@quim.ucm.es (R. Sáez-Puche).

0022-4596/$ - see front matter © 2006 Elsevier Inc. All rights reserved.
doi:10.1016/j.jssc.2006.09.025

[3] and more recently by Woodward [4]. Because nitrogen and oxygen play the same role in the anionic network, some of these quaternary oxynitrides show the same crystal structures than the corresponding ternary oxides [5].

In this framework, we have focused on the rare-earth tungstates $RWO_3N$ ($R$ = rare earth) recently investigated by Marchand et al. [6,7] and it has been reported that $RWO_3N$ ($R$ = Pr, Nd, Sm, Gd and Dy) have been prepared as new phases which crystallize with the tetragonal scheelite-type structure where oxygen and nitrogen are randomly distributed within the anionic sublattice. In the case of the LaW(O, N)$_3$ was obtained as a tetragonal perovskite, where the formal oxidation state of tungsten is lower than VI and electrical measurements have shown the semiconductor behavior of this material [8].

This paper aims the synthesis, structural characterization and the study of the magnetic properties of $R$–W–O–N oxynitrides, where $R$ is Nd and Eu.

## 2. Experimental

Precursor $R_2W_2O_9$ oxides were prepared heating in air stoichiometric amounts of $R(NO_3)_3 \cdot 6H_2O$ nitrates, with $R$ = Nd and Eu, and tungsten trioxide for 48 h at 1243 K with one interruption for grinding in order to homogenize and enhance the reaction products.

Samples in the system $R$–W–O–N ($R$ = Nd and Eu) were obtained by the nitridation reaction of the corresponding $R_2W_2O_9$ oxides with flowing ammonia during 24 h and at temperatures of 1073 K. In fact at this temperature only the NdW(O, N)$_4$ has been obtained as pure phase; in the case of Europium compound both a scheelite EuW(O, N)$_4$ and a perovskite phase EuW(O, N)$_3$ were observed. The preparation of this latter oxynitride as single phase has been achieved by a further thermal treatment under ammonia flow up to 1173 K for 24 h. The two oxynitrides obtained show a black colour. The nitrogen amount was determined by the method of inert gas fusion with a LECO TC-500 analyzer [9]. After thermal decomposition of the samples in graphite furnace under helium atmosphere, the oxygen content was determined by measuring the $CO_2$ concentration (after oxidation of CO) with an IR-cell. Analysis of the nitrogen was carried out by measuring the thermal conductivity of the mixture of helium and nitrogen gas after absorption of the $CO_2$. At least three analyses were performed in the same conditions for each sample in order to get a more accuracy in the determined composition.

Polycrystalline oxides used as precursors and obtained oxynitrides were analyzed by X-ray powder diffraction. Measurements were carried out on a Philips X'Pert MPD diffractometer, with Ni filtered Cu $K_\alpha$ radiation. A step scan of 0.04° $2\theta$ in the range 10–120° and a counting time of 15 s for each step were employed. Starting lattice parameters to be used in Rietveld profile refinements using the WinPLOTR program [10] have been obtained from the X-ray diffraction data refined with the checkcell software program.

Magnetic susceptibility measurements were performed in a Quantum Design XL-SQUID magnetometer at 1000 Oe between 1.9 and 300 K.

## 3. Results and discussion

### 3.1. Chemical and structural characterization

X-ray diffraction data of the precursor $R_2W_2O_9$ (La–Eu) oxides reveal that they are pure phases, which crystallize with monoclinic symmetry, S.G $P2_1/c$ according to the data previously reported by Mc. Carthy [11]. The nitridation of these $R_2W_2O_9$ oxides, with $R$ = (Nd and Eu), yields the formation of the corresponding oxynitrides as single phases using the synthesis conditions given in the Section 2.

Chemical analysis results determined by the method of hot gas extraction (LECO) [9] are shown in Table 1. The experimental formulae are obtained by taking into account the nitrogen and oxygen content and yield mixed valence compounds where the tungsten shows 5+ and 6+ as valence states and neodymium and europium show the 3+ and 2+ oxidation state respectively. These oxidation states agree with the experimental values determined from the magnetic susceptibility and magnetization measurements we will discuss below.

After identification of the crystalline phase, the Rietveld profile analysis for the Nd-containing oxynitride was performed in the tetragonal S.G. $I4_1/a$ (# 88) using as starting values these previously refined for the unit-cell and positional parameters reported for the isostructural $CaWO_4$ [12]. The phase was well crystallized, see Fig. 1, and the refined unit-cell dimensions (Å), were $a = 5.255(1)$ and $c = 11.399(3)$, that is, slightly larger than in the scheelite structure-type $CaWO_4$ oxide. Refined atomic coordinates and calculated main interatomic distances are given in Table 2.

Fig. 2 shows the $bc$ perspective of the scheelite-type tetragonal structure of $NdWO_{3.05}N_{0.95}$. This structure is constituted by chains along a and b directions of alternate Nd(O,N)$_8$ bisdisphenoids and W(O, N)$_4$ tetrahedra, which are sharing edges, whereas in the $c$ direction Nd(O,N)$_8$ of two consecutive chains are connected sharing one edge, forming dimers of bisdisphenoids $Nd_2(O,N)_{14}$. The main bond lengths obtained for this oxynitride are collected in Table 2.

On the other hand, the Eu oxynitride presents the cubic perovskite-type structure, S.G. $Pm\bar{3}m$ with refined unit cell

Table 1
Experimental nitrogen content in $R$-oxynitrides, $R$ = Nd and Eu

| Composition | Nexp (wt%) | N(mol) | Exp. Formulation |
|---|---|---|---|
| NdW(O,N)$_4$ | 3.41 | 0.95 | $NdWO_{3.05}N_{0.95}$ |
| EuW(O,N)$_3$ | 5.2 | 1.42 | $EuWO_{1.58}N_{1.42}$ |

parameter $a = 3.976(3)$ Å, see Table 2 and Fig. 3. The experimental bond distance of 2.811 Å for the Eu-(O, N) is closer to the sum of the ionic radius of $Eu^{2+}$ (1.25 Å) and $O^{2-}$ (1.38 Å)/$N^{3-}$ (1.46 Å) than when $Eu^{3+}$ (1.02 Å) is considered.

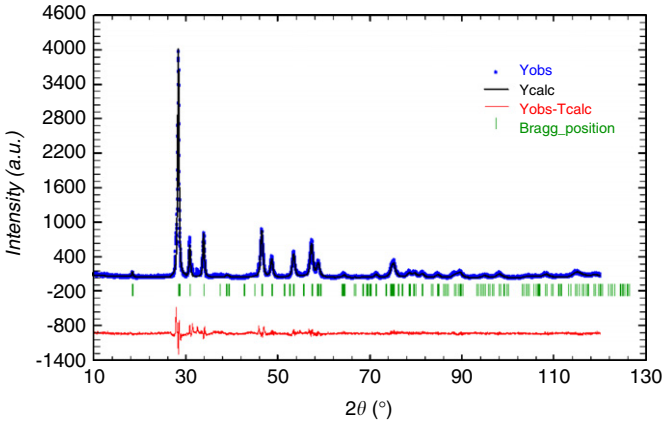


Fig. 1. Experimental (dots) and refined (solid line) X-ray diffraction patterns for oxynitride $NdWO_{3.05}N_{0.95}$. Vertical marks show the position of the allowed reflections. The lower curve below pattern represents the difference between the observed pattern and the calculated Rietveld refinement profile.

Table 2
Rietveld refinement details, unit-cell parameters, atomic coordinates and main interatomic distances in $NdWO_{3.05}N_{0.95}$ and $EuWO_{1.58}N_{1.42}$ oxynitrides

| | | $NdWO_{3.05}N_{0.95}$ | $EuWO_{1.58}N_{1.42}$ |
|---|---|---|---|
| Space group | | $I4_1/a$ | $Pm\bar{3}m$ |
| Unit cell dimensions | | $a = 5.255(1)$ | $a = 3.976(3)$ |
| | | $c = 11.399(1)$ | |
| Volume (Å$^3$) | | 314.7(8) | 62.9(5) |
| $R_B$ | | 5.3 | 4.9 |
| $R_F$ | | 6.7 | 3.9 |
| Site, $x$, $y$, $z$ ($\times 10^3$) | $R$ | 4$b$, 0, $\frac{1}{4}$, $\frac{5}{8}$ | 0, 0, 0 |
| | $W$ | 4$a$, 0, $\frac{1}{4}$, $\frac{1}{8}$ | $\frac{1}{2}$, $\frac{1}{2}$, $\frac{1}{2}$ |
| | O/N | 16$f$, 150(4), 80(5), 211(1) | 0, $\frac{1}{2}$, $\frac{1}{2}$ |
| $B_{ov}$ | | 0.67(2) | 0.26(1) |
| Main distances (Å) | $R$-(O/N) | $2.481(2) \times 4$ | $2.811(5) \times 12$ |
| | $R$-(O/N) | $2.470(3) \times 4$ | |
| | $W$-(O/N) | $1.808(1) \times 4$ | $1.988(4) \times 6$ |

From the X-ray diffraction data, we were not able to determine whether there was ordering between the oxygen and nitrogen atoms, because of their almost identical scattering factors. Further structural studies would need to be undertaken, using neutron diffraction, which would allow any anionic ordering to be highlighted due to different nuclear scattering lengths for oxygen and nitrogen ($b$(O) = 5.80 fm, $b$(N) = 9.36 fm).

### 3.2. Magnetic properties

Magnetic properties of the oxynitrides $NdWO_{3.05}N_{0.95}$ and $EuWO_{1.58}N_{1.42}$, have been studied from the magnetization and magnetic susceptibility measurements. Fig. 4 shows the temperature dependence of the magnetic susceptibility for $NdWO_{3.05}N_{0.95}$ in an applied field of 1 kOe. The experimental susceptibility $\chi$ follows a Curie–Weiss law, $\chi_m^{-1} = 22.3(1) + 0.5682(8)$ T mol emu$^{-1}$, in a very wide temperature range 50–300 K. The effective paramagnetic moment results to be 3.75 $\mu_B$, Table 3, somewhat higher than the expected value for $Nd^{3+}$ free-ion, and thus indicative of the some additional paramagnetic contribution from tungsten, partially reduced from $W^{6+}$ to $W^{5+}$, which moreover justifies the black colour that presents this oxynitride. The downward deviation from the Curie–Weiss law below 50 K, evident in Fig. 4, and the Weiss constant $\theta = -39.3$ K are attributed as due to the $Nd^{3+}$ low-lying crystal field CF $^4I_{9/2}$ energy levels becoming depopulated at low temperatures. In order to rationalize this attribution, the calculation of the paramagnetic susceptibility using semi-empirical structure-derived CF parameters will be presented in the next section.

Fig. 5 shows the thermal variation of the magnetic susceptibility of $EuWO_{1.58}N_{1.42}$. This plot displays a ferromagnetic-like increase in the susceptibility with a Curie temperature around 20 K. Fitting the high-temperature susceptibility data between 30 and 300 K, Fig. 5 inset, to the Curie–Weiss law gives as results values of the effective magnetic moment $\mu_{eff} = 8.01\,\mu_B$ and $\theta = 73$ K, which is in good agreement with the calculated value (7.94 $\mu_B$) taking into account that the europium and

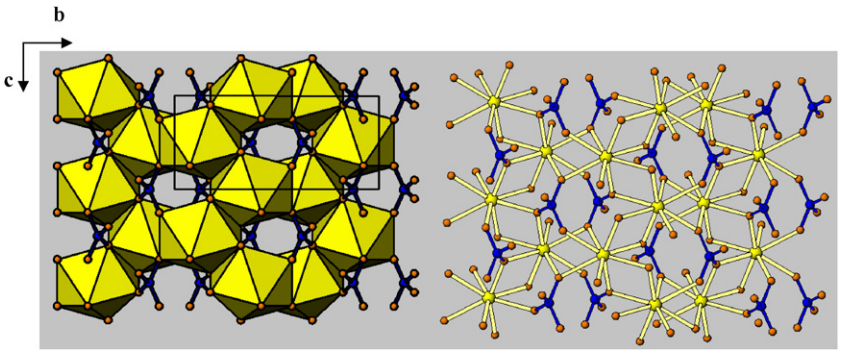


Fig. 2. $bc$ view of the $Nd(O,N)_8$ (yellow) and $W(O, N)_4$ (blue) coordinations in $NdWO_{3.05}N_{0.95}$. Dimeric units $(Nd)_2(O, N)_{14}$ are lying along the $c$-axis.

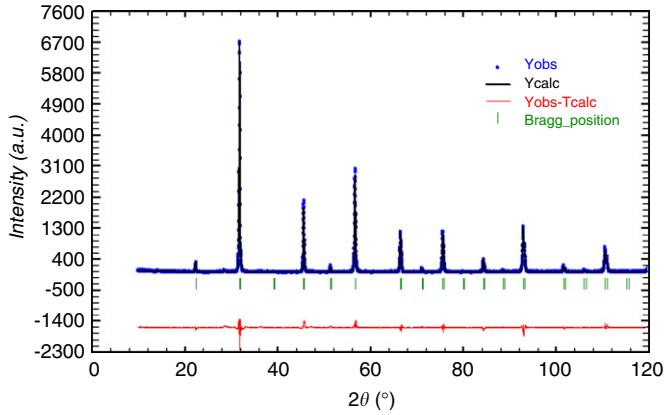


Fig. 3. Experimental (dots) and refined (solid line) X-ray diffraction patterns for oxynitride $EuWO_{1.58}N_{1.42}$. Vertical marks show the position of the allowed reflections. The lower curve below pattern represents the difference between the observed pattern and the calculated Rietveld refinement profile.

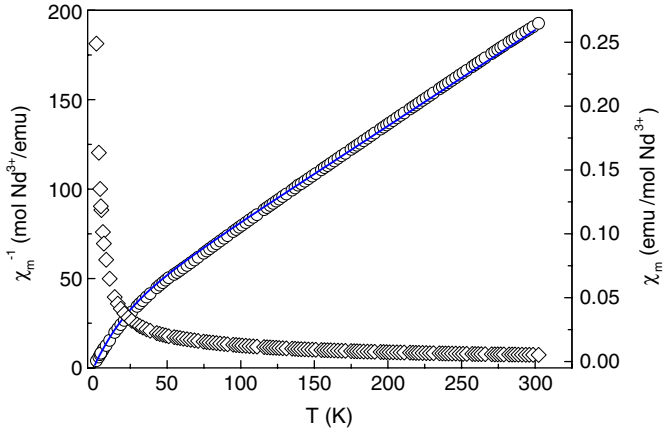


Fig. 4. Variation of magnetic susceptibility with temperature for $NdWO_{3.05}N_{0.95}$ Open symbols are the experimental data and solid line represents the simulated susceptibility using the SOM method.

Table 3
Magnetic parameters, effective magnetic moment ($\mu_{eff}$), Curie temperature ($T_c$) and saturation moment ($\sigma_s$) obtained for $NdWO_{3.05}N_{0.95}$ and $EuWO_{1.58}N_{1.42}$ oxynitrides

| Compound | $\mu_{exp}/\mu_B$ | $\mu_t/\mu_B$ | $\theta/K$ | $\sigma_s/\mu_B$ | $B_r/\mu_B$ | $H_c/O_e$ | $T_c/K$ |
|---|---|---|---|---|---|---|---|
| $NdWO_{3.05}N_{0.95}$ | 3.75 | 3.62 | —39.3 | — | — | — | — |
| $EuWO_{1.58}N_{1.42}$ | 8.01 | 7.94 | 73 | 6.00 | 0.50 | 150 | 20 |

tungsten present in the $EuWO_{1.58}N_{1.42}$ compound have the oxidation states of 2+ and 5+, respectively. The magnetic field dependence of the magnetization for this oxynitride at different temperatures is shown in Fig. 6. The $M$ vs. $H$ curves show the typical behavior of a ferromagnetic compound and tend to saturate with a value of $6\,\mu_B$ at 5 T in the case of the curve measured at 2 K. By contrast, at 30 K the straight line obtained could be explained taking into account that this compound at this temperature

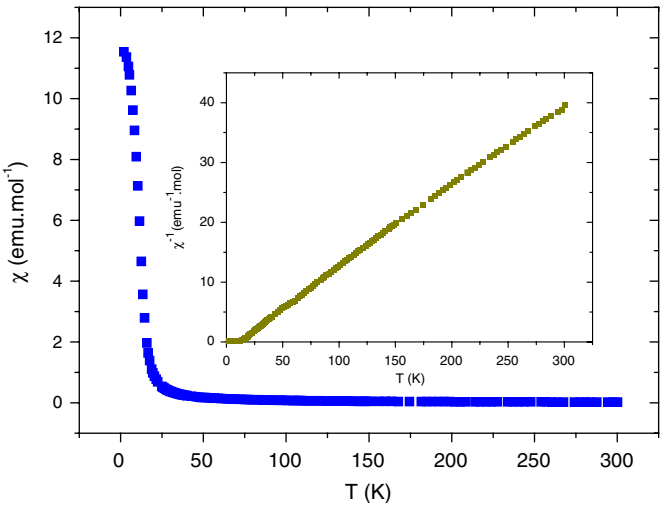


Fig. 5. Variation of magnetic susceptibility with temperature for $EuWO_{1.58}N_{1.42}$. The inset is the $\chi^{-1}$ versus $T$.

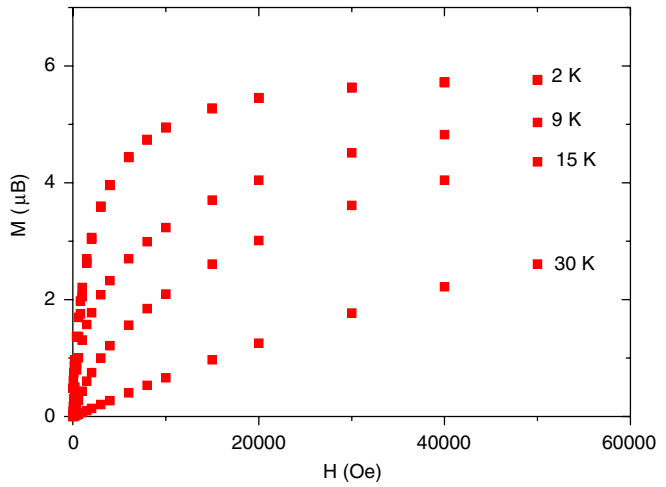


Fig. 6. Magnetization vs magnetic field plot of the $EuWO_{1.58}N_{1.42}$ oxynitride at different temperatures in the range 0–5 T.

behaves as paramagnetic since the determined Curie temperature is 20 K. Fig. 7 shows the hysteresis loop obtained at 2 K where the remanence takes a value of $0.50\,\mu_B$; while the coercitive field is as low as 150 Oe, which yields at this compound a soft magnetic character. This behavior can be explained taking into account the different pathways throughout the superexchange magnetic interactions take place. Since this oxide crystallizes with the undistorted perovskite structure there are two main pathways in which both W and Eu are involved, W–O–W with an angle of 180° and W–O–Eu at 90°. It is worth noting that since, about 50% of the tungsten cations are diamagnetic ($W^{6+}$) superexchange W–O–W interactions will be diminished and the main interaction should takes place between the $t_{2g}^1$ and the half filled $4f^7$ orbitals of tungsten and europium, respectively. This gives rise to an antiferromagnetic coupling between the $W^{5+}$ and $Eu^{2+}$

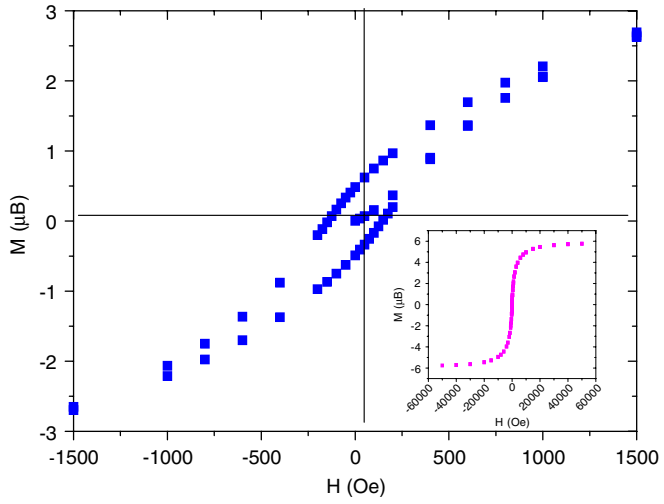


Fig. 7. Hysteresis loops at 2 K. The inset is the hysteresis loop at 2 K for a magnetic field between −5 and 5 T.

sublattices. This results in a very poor d–f orbital overlap, which is consistent with low $T_c$ being 20 K.

On the other hand, the saturation moment of 6 $\mu_B$ agrees well with the colineal antiparallel arrangement between the $Eu^{2+}$ magnetic moment of 7 $\mu_B$ and the 1 $\mu_B$ assigned to $W^{5+}$, which has one unpaired electron giving rise an overall ferrimagnetic behavior with a saturation magnetic moment of 6 $\mu_B$ for this new oxynitride.

### 3.3. Paramagnetic susceptibility simulation from crystal field effects on $NdWO_{3.05}N_{0.95}$

A way to test the CF origin of the observed low temperature bending in the $\chi_m$ vs. $T$ curve for $R$-compounds is to perform this calculation using the van Vleck formalism [13], based on configuration wavefunctions derived from a CF analysis:

$$\chi_i = N\beta^2 \sum_a \left[ \frac{\langle \phi_a | (L + g_e S)u | \phi_a \rangle^2}{kT} - 2 \sum_b \frac{\langle \phi_a | (L + g_e S)u | \phi_b \rangle \langle \phi_b | (L + g_e S)u | \phi_a \rangle}{E_a - E_b} \right] \times B_a,$$

where $N$ is the Avogadro's number, $\beta$ the Bohr magneton, $k$ the Boltzmann constant, $E$ and $\phi$ the non-perturbed by the magnetic field energy levels and wavefunctions, respectively, described on the $|SLJM_J\rangle$ basis, and $L + g_e S$ is the component (i) of the magnetic interaction associated to a tensorial operator of rank 1, the magnetic dipole operator, $g_e$ is the gyromagnetic ratio (2.0023), being $\boldsymbol{u}$ the unitary vector corresponding to the $i$ axis. The sums run over thermally populated levels, according to the thermal partition law $B_a = \exp(-E_a/kT)/\Sigma_a \exp(-E_a/kT)$. The different values of the tensor components, or combinations of them, destroy the isotropy observed for the free-ion or even for an ion in a cubic symmetry. The anisotropy components are called $\chi_\parallel$ (component 0 of the tensor) and $\chi_\perp$ (components $\pm 1$ of the tensor). In that expression the matrix elements are calculated using the Racah algebra rules.

The formula is the sum of a temperature-dependent diagonal energy term that normally produce first order Zeeman splitting, and a temperature-independent off diagonal term, a result of the second-order perturbation, which is reminiscent of the classical Curie–Weiss law.

Since no phenomenological CF parameters are available, we have applied the semi-empirical Simple Overlap Model SOM [14,15] that calculates these parameters from the structural data of the compound. SOM considers effective charges, located around the middle of the $Nd^{3+}$–Ligand L (O/N) distances, which are assumed to be proportional to the magnitude of the overlap integral $\rho$ between the $4f$ and the valence orbitals of $Nd^{3+}$ and L (O/N), respectively. The CF parameters are written as

$$B_q^k = \langle r^k \rangle \sum_L \rho_L \left( \frac{2}{1 \pm \rho_L} \right)^{k+1} A_q^k(L), \quad \rho_L = \rho_0 \left( \frac{R_0}{R_L} \right)^{3.5}.$$

The sum over $L$ is restricted to the first coordination sphere, consequently the required crystallographic data are restricted to the closest O/N positions and thus $\langle r^k \rangle$ radial integral are not corrected from the spatial expansion. $\rho$ varies for each $L$ as a function of the distance $R$, according to the exponential law above indicate, $R_0$ being the shortest distance. $A_q^k$ is the lattice sum and it takes into account the symmetry properties of the $R^{3+}$ site, including the effective charge attributed to $L$. The sign $\pm$ of the denominator stands for differentiating the type of $L$: when a single type of $L$ is considered, a minus sign corresponding to the normal shift of the charge barycentre from the mid-point of the $R$ bonding distance should be taken, and when different $L$ are present the minus sign corresponds to the most covalent one.

Crystallographic data for $NdWO_{3.05}N_{0.95}$ were those from our previous X-ray analysis, the mean effective charge for O/N was taken as −0.8 and $\rho$ was adjusted to a value of 0.05, intermediate between typical values for $4f^N$ configurations, 0.04 (mostly ionic compounds) and 0.08 (mostly covalent compounds) [16]. Results of simulated $S_4$ SOM CF parameters are ($cm^{-1}$) $B_0^2 = 547$, $B_0^4 = -823$, $B_4^4 = \pm 805$, $B_0^6 = -207$, $B_4^6 = \pm 988$ and $iB_4^6 = \pm 208$.

The calculation of $\chi_m$ and its variation with temperature for the $S_4$ $Nd^{3+}$ in $NdWO_{3.05}N_{0.95}$ was carried out with the above CF parameters and free-ion parameters from $Nd^{3+}$ in the also scheelite structure-related $AgNd(WO_4)_2$ [17] crystal, an appropriate choice taking into account that their differences are predicted to be weak, using the program IMAGE [18].

The comparison between experimental and calculated curves of the variation of the $\chi_m^{-1}$ with the temperature for $NdWO_{3.05}N_{0.95}$ is plotted in Fig. 4. A very satisfactory concordance that extends over the entire measured temperature range is found between both curves, being especially well reproduced the bending at low temperature.

## 4. Conclusions

Oxynitrides $NdWO_{3.05}N_{0.95}$ and $EuWO_{1.58}N_{1.42}$ have been synthesized by the nitridation of $R_2W_2O_9$ oxides, $R = Nd$ and Eu at 1173 K. The neodymium oxynitride crystallizes with the scheelite type structure, while the $EuWO_{1.58}N_{1.42}$ derivative presents the cubic perovskite type. Magnetic properties of both $NdWO_{3.05}N_{0.95}$ and $EuWO_{1.58}N_{1.42}$ oxynitrides show very interesting f eatures.

The neodymium derivate behaves as paramagnetic in a wide range of temperature 50–300 K. The downward deviation from the Curie–Weiss behavior below 50 K has been simulated taking into account the splitting of the $^4I_{9/2}$ ground term under crystal field influence of $S_4$ symmetry, using the semiempirical SOM method.

Whereas the europium oxynitride is paramagnetic down 20 K. Below this temperature the sudden jump observed in the magnetic susceptibility at 20 K and the hysteresis loops measured below the Curie temperature are indicative of the onset of magnetic interactions in which the $Eu^{2+}$ and $W^{5+}$ sublattices are ferrimagnetically ordered.

## Acknowledgments

The authors would like to acknowledge the financial support from the CICYT to the project MAT2003-08465-C02-01. Thank also due to M[a]Jesús Sánchez García and Antonio Rodriguez Jimenez of the Institute of Ceramics and Glass of CSIC, Department of Physics and Chemistry of Surface and Processes, for the analysis of the samples.

## References

[1] N. Diot, R. Marchand, J. Haines, J.M. Leger, P. Macaudière, S. Hull, J. Solid State Chem. 146 (1999) 390–393.
[2] M. Pérez-Estébanez, R. Pastrana-Fábregas, J. Isasi-Marín, R. Sáez-Puche, J. Mater. Res. 21 (2006).
[3] R. Marchand, Ternary and higher order nitride materials, in: K.A. Geschneidner, L. Eyring (Eds.), Handbook on the Physics and Chemistry of Rare Earths, Vol. 25, Elservier Science, New York, 1998 (Chapter 166).
[4] Young-Ill Kim, Thesis. Synthesis, crystal structures and dielectric property of oxynitrides perovskite. The Ohio State University, 2005.
[5] F. Tessier, R. Marchand, J. Solid State Chem. 171 (2003) 143–151.
[6] P. Antonie, R. Marchand, Y. Laurent, Rev. Int. Hautes. Temper. Refract. Fr. 24 (1987) 43.
[7] F. Cheviré, F. Tessier, R. Marchand., Mater. Res. Bull. 39 (2004) 1091–1101.
[8] P. Bacher, P. Antonie, R. Marchand, P.L. Harindon, Y. Laurent, G. Roult, J. Solid State Chem. 77 (1988) 67.
[9] http://www.lecoinstrumentos.es.
[10] T. Roisnel and J. Rodriguez Carvajal, WinPLOTR, plotr@llb.saclay.cea.fr, http://www-llb.cea.fr/fullweb/winplotr/winplotr.htm.
[11] G.J. Mc. Carthy, R.D. Fisher, G.G. Johnson, C.E. Gooden, Nat. Bur. Standards Spec. Publ. 364 (1972) 397.
[12] R.M. Hazen, L.W. Finger, J.W.E. Mariathasan, J. Phys. Chem. Solids. 46 (1985) 253.
[13] J.H. Van Vleck, J. Appl. Phys. 39 (1968) 365;
J.H. Van Vleck, The Theory of the Electric and Magnetic Susceptibilities, Oxford University Press, London, 1932.
[14] O.L. Malta, Chem. Phys. Lett. 88 (1982) 353.
[15] P. Porcher P, M. Couto dos Santos, O. Malta, Phys. Chem. Chem. Phys. 1 (1999) 397.
[16] O.L. Malta, H.J. Batista, L.D. Carlos, Chem. Phys. 282 (2002) 21.
[17] C. Colón, A. Alonso Medina, F. Fernández, R. Sáez Puche, V. Volkov, C. Cascales, C. Zaldo, Chem. Mater. 17 (2005) 6635.
[18] P. Porcher, Fortran routines REEL and IMAGE for simulation of $d^N$ and $f^N$ configurations involving real and complex crystal field parameters, 1989, unpublished. See, for instance, C. Zaldo, M. Rico, C. Cascales, M.C. Pujol, J. Massons, M. Aguiló, F. Diaz, P. Porcher, J. Phys.: Condens. Mat. 12 (2000) 8531.